DOI: 10.1002/asia.200600306

Superoxide Compounds of the Large Pseudo-Alkali-Metal Ions Tetramethylammonium, -Phosphonium, and -Arsonium

Pascal D. C. Dietzel,[b] Reinhard K. Kremer,[a] and Martin Jansen*[a]

Abstract: Compounds of the three large cations tetramethylammonium, tetramethylphosphonium, and tetramethylarsonium with the superoxide radical anion were synthesized by either metathesis or ion exchange in liquid ammonia. They were obtained from concentrated solutions as ammoniates in the form of long needle-shaped single crystals. $[N(CH_3)_4](O_2)\cdot 3NH_3$ crystallizes in the monoclinic crystal system, whereas the two compounds $[E(CH_3)_4](O_2)\cdot 2NH_3$ (E = P, As) are isostructural and belong to the orthorhombic crystal system. The cation–anion packing in all three crystal structures is related to the sodium chloride structure. All structures contain hydrogen bonds between the ammonia molecules and between ammonia and the superoxide. The solvent of crystallization was easily released from the crystals upon complete removal of the solvent from the reaction vessel, leading to polycrystalline samples. The Raman spectra of all three solvent-free compounds show the symmetric stretching mode of the superoxide ion at about 1123 cm^{-1}. The desolvated $[N(CH_3)_4](O_2)$ was investigated by powder X-ray diffraction, and the crystal structure was solved by ab initio simulated annealing methods by using rigid-body models of the constituent molecular ions. The superoxide ion shows rotational disorder. The magnetic susceptibility of tetramethylammonium superoxide follows the Curie–Weiss law with a high-temperature effective magnetic moment of 1.66(3) μ_B and a paramagnetic Curie temperature of $\Theta = -13(6)$ K. Complementary electron paramagnetic resonance spectroscopy revealed that the average g factor is temperature-dependent. It decreased from 2.15 at 10 K to 1.66 at 100 K, possibly due to the onset of rotational motion of the superoxide ion and in accordance with the lower-than-expected effective magnetic moment.

Keywords: EPR spectroscopy · ion exchange · magnetic properties · Raman spectroscopy · superoxides · X-ray diffraction

Introduction

The superoxide ion is of special interest for various reasons. For the organic chemist, it is very useful as a unique redox reagent. In biochemistry, it is of particular importance because of its crucial role in numerous biological processes. Here, the superoxide ion is usually bound to a metal atom; therefore, transition-metal complexes with superoxide as a ligand have been widely studied in the past.[1–5] In inorganic chemistry, the superoxide ion is of interest because it belongs to a limited number of paramagnetic main-group molecules. So far, much less research has been done on compounds that contain the superoxide ion as an isolated moiety than on its complexes. To a large extent, this seems to be due to the paucity of isolable superoxide compounds. The only thermodynamically stable representatives among these are the binary superoxides of the heavier alkali metals potassium, rubidium, and cesium.[6–8] Even these compounds are chemically very delicate as they readily react, for example, with moisture or carbon dioxide, and consequently, all handling has to be done under inert-gas conditions. Nevertheless, superoxides of the heavier alkali metals appear to be best-suited to the study of the properties of the superoxide ion because of their relative easy accessibility.[9–48]

The focus of previous work was on the crystal structures of the alkali-metal superoxides.[9,12,14–16,20,34] In the course of these investigations, it was shown that all these superoxides undergo several successive structural phase transitions on changes in temperature. The respective crystal structures

[a] Dr. R. K. Kremer, Prof. Dr. M. Jansen
Max-Planck-Institut für Festkörperforschung
Heisenbergstr. 1, D-70689 Stuttgart (Germany)
Fax: +49-711-6891502
E-mail: M.Jansen@fkf.mpg.de

[b] Dr. P. D. C. Dietzel
SINTEF Materials and Chemistry
Pb. 124 Blindern, N-0314 Oslo (Norway)
and
Centre of Materials Science and Nanotechnology
Department of Chemistry, University of Oslo (Norway)

differ mainly in the way in which the dumbbell-shaped superoxide ions rearrange within the voids that result from the packing of the large spherical alkali-metal cations. The occurrence of these phase transitions and concomitant static or dynamic disorder has severely hampered the investigation of most of the basic physical properties of the superoxide ion. For instance, the determination of the bond length of the superoxide notoriously suffers from rotational-disorder phenomena in the higher-temperature phases or from twinning, which results when this rotational motion is frozen on cooling. Also, the magnetic moments of the different phases have been shown to vary significantly.[29] In part, the uncertainties may be due to the fact that some of the phases exist only in a very narrow temperature range, which may affect the accuracy in determining the effective magnetic moments. Moreover, because of short nearest-neighbor distances between adjacent superoxide ions, intermolecular interactions between the superoxide ions are no longer negligible. Thus, it would be beneficial to have access to new compounds that contain the superoxide ion but do not show the disadvantageous features mentioned above. Good candidates that possibly serve this purpose may be the superoxides of tetraorganylonium ions. Even the smallest of these, the tetramethylammonium ion, which has a thermochemical radius of 2.34 Å,[49] is larger than the cesium cation. A larger cation radius should result in a larger anion–anion distance, which should eventually reduce the intermolecular interaction of the paramagnetic anions. In fact, a number of tetraalkylammonium superoxides have been known for some time.[50–53] Tetramethylammonium superoxide has even been used in chemical reactions, for example, as a starting material for preparing tetramethylammonium ozonide by metathesis[54,55] or other tetraorganylammonium superoxides by ion exchange.[56,57] Previous investigations have not yielded a definite answer regarding the crystal structure of tetramethylammonium superoxide.[60] Herein we report our results on tetramethylammonium superoxide and its higher homologues, tetramethylphosphonium and tetramethylarsonium superoxide. We show that the ion-exchange reaction that has so far been restricted to the synthesis of tetraorganylammonium compounds also applies to the synthesis of quaternary organic phosphonium and arsonium compounds.

Results and Discussion

Syntheses

Liquid ammonia is the solvent of choice for all reactions involving the superoxide ion in solution. It is sufficiently polar to dissolve many salts of monovalent cations and anions, and its high basicity prevents the protonation and subsequent instantaneous decomposition of a number of labile anions such as the superoxide ion.[61,62] Potassium superoxide, which is easily obtained from the pure alkali metal and oxygen, is the starting material for all subsequent syntheses of superoxide compounds. However, because of its low solubility in liquid ammonia, the efficient ion-exchange route cannot be employed to convert it directly into the desired superoxide compounds. Tetramethylammonium superoxide, on the other hand, readily dissolves in liquid ammonia.[50,51] It was prepared in a mechanochemical metathesis reaction by milling tetramethylammonium hydroxide monohydrate and potassium superoxide.[50,52,53] Among the compounds present in the reaction mixture, tetramethylammonium superoxide was the most soluble in liquid ammonia and therefore could be extracted and harvested by recrystallization with intermittent filtration. Long colorless needles crystallized from concentrated solutions of tetramethylammonium superoxide in liquid ammonia (**1a**). Tetramethylphosphonium superoxide (**2**) and tetramethylarsonium superoxide (**3**) were synthesized from tetramethylammonium superoxide by ion exchange in liquid ammonia. The crystals obtained from concentrated solutions were colorless and needle-shaped. After the mother liquor was completely removed, single crystals of **1a**, **2**, and **3** disintegrated into finely divided colorless to pale-yellow, opaque substances. This observation strongly indicates that the large needles initially obtained contained solvent molecules. The general route for the synthesis of tetraorganylonium superoxide compounds is illustrated in Scheme 1. All measurements of the physical properties of tetramethylammonium superoxide were performed on the desolvated compound (**1b**).

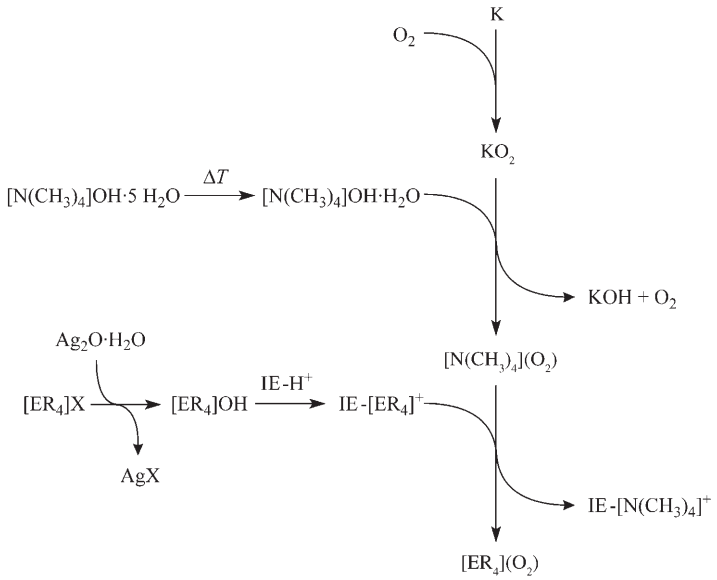

Scheme 1. Route for the synthesis of the tetraorganylonium superoxide compounds. IE = ion-exchange resin, E = N, P, or As, X = Cl, Br, or I, R = CH_3.

Crystal Structures

Table 1 contains details of the data collection and structure refinements of compounds **1a**, **2**, and **3**. Selected geometric parameters are listed in Table 2. The results of the single-crystal structure analyses confirm the presence of ammonia molecules in all three structures. The distances and angles in

Table 1. Summary of crystallographic data for **1a**, **2**, and **3**.

	1a	**2**	**3**
Formula	$[N(CH_3)_4](O_2)\cdot 3NH_3$	$[P(CH_3)_4](O_2)\cdot 2NH_3$	$[As(CH_3)_4](O_2)\cdot 2NH_3$
Formula weight [g mol^{-1}]	157.25	157.17	201.12
T [K]	100	100	100
Space group	$P2_1/n$	$Cmc2_1$	$Cmc2_1$
Z	4	4	4
a [Å]	8.3400(13)	9.299(11)	9.2877(12)
b [Å]	8.3747(13)	14.925(18)	14.8260(19)
c [Å]	13.850(2)	6.807(8)	6.7628(9)
β [°]	92.024(3)	90	90
V [Å^3]	966.7(3)	944.8(19)	931.2(2)
λ [Å]	0.71073	0.71073	0.71073
ρ_{calcd} [g cm^{-3}]	1.080	1.105	1.435
μ [mm^{-1}]	0.084	0.242	3.600
Crystal size [mm^3]	$0.05\times0.05\times0.01$	$0.10\times0.10\times0.020.50\times0.20\times0.10$	
F(000)	356	348	420
2θ range [°]	5.62–50.14	5.16–54.0	5.18–68.00
Reflections measured	5906	3878	6079
Unique reflections	1692	1108	1974
R_{int}	0.0418	0.1097	0.0326
Observed reflections	1180	872	1921
Reflections used in refinement	1692	1108	1974
Parameters/restraints	175/0	81/18	82/9
R_1 ($I>2\sigma(I)$)	0.0396	0.0545	0.0276
wR_2 (all data)	0.1033	0.1217	0.0663
GOF	1.001	1.032	1.128
Final difference peaks [e Å^{-3}]	−0.126/0.196	−0.260/0.526	−1.255/1.205

Table 2. Selected bond lengths and angles for **1a**, **2**, and **3**.

	1a	**2**	**3**
d(E−C(Me)) [Å]	1.487(2), 1.488(2), 1.491(2), 1.492(2)	1.761(1), 1.777(6), 1.778(4) (×2)	1.878(3), 1.890(2) (×2), 1.893(3)
∢(C(Me)−E−C(Me)) [°]	108.6(2), 109.3(2) (×2), 109.4(2), 109.9(2), 110.4(2)	108.6(2) (×2), 108.9(2), 109.8(3), 110.4(2) (×2)	107.8(1) (×2), 109.5(2), 109.7(2), 110.9(1) (×2)
d(O−O) [Å]	1.318(2)	1.315(5)	1.320(3)

solid ammonia[63] were used to analyze the hydrogen-bonding network among the ammonia molecules and the superoxide ions in **1a**, **2**, and **3**, and the respective intermolecular distances are listed in Table 3.

In the crystal structure of **1a**, the tetramethylammonium and superoxide ions aggregate into layers oriented parallel to [010], whereas the ammonia molecules are inserted between these layers (Figure 1a). Adjacent layers are stacked in such a way that the packing of the cations and anions resembles that of the sodium chloride structure.

The ammonia molecules engage all of their hydrogen atoms in hydrogen bonds with each other and to the superoxide ions, thus forming a three-dimensional network of hydrogen bonds wrapped around the cations. The substructure formed by the ammonia consists of undulating strands along [010], which are made up of *trans* edge-connected tetragons of ammonia molecules (Figure 1b). Adjacent one-dimensional ammonia ribbons are linked through superoxide ions to form sheets between the cation layers of the crystal structure.

Compounds **2** and **3** are isostructural. Again, the packing of cations and anions is reminiscent of the sodium chloride structure, and there are solvent ammonia molecules interspersed between the layers of the ions (Figure 2). The ammonia molecules are linked to each other to form chains by each acting as donor and acceptor for one hydrogen bond. Two of these chains are then linked by hydrogen bonds to superoxide ions, for which the ammonia molecule utilizes its two remaining hydrogen atoms. One of these bonds points to a superoxide above the plane of the resulting double chain of ammonia molecules, the other points to the one below. Unlike **1a**, the hydrogen bonds do not form a three-dimensional network. This seems to be attrib-

Table 3. Short intermolecular distances (<3.4 Å) that indicate possible hydrogen bonds in **1a**, **2**, and **3**.

D−H···A	d(D−H) [Å]	d(H···A) [Å]	d(D···A) [Å]	∢(D−H···A) [°]
1a				
N2−H1N···O2	0.898(19)	2.401(19)	3.294(2)	172.4(15)
N2−H2N···N4	0.90(2)	2.46(2)	3.349(2)	169.0(15)
N2−H3N···O2	0.86(2)	2.29(2)	3.145(2)	177.7(17)
N3−H4N···O2	0.86(2)	2.35(2)	3.201(2)	170.7(19)
N3−H5N···O2	0.91(2)	2.48(2)	3.390(2)	173.8(16)
N3−H6N···N4	0.88(2)	2.51(2)	3.375(2)	167.4(15)
N4−H7N···N2	0.884(18)	2.383(19)	3.245(2)	165.0(15)
N4−H8N···N3	0.890(19)	2.41(2)	3.289(2)	168.8(17)
N4−H9N···O1	0.94(2)	2.23(2)	3.164(2)	169.8(14)
C2−H5···O2	0.952(18)	2.434(19)	3.363(3)	165.3(14)
2				
N1−H4A···N1	0.92(2)	2.60(3)	3.414(4)	147(3)
N1−H4B···O2	0.92(2)	2.35(2)	3.248(5)	166(4)
N1−H4C···O1	0.92(2)	2.31(2)	3.224(5)	173(4)
N1−H4C···O2	0.92(2)	2.52(3)	3.370(5)	154(4)
C1−H1A···O1	0.899(19)	2.60(3)	3.354(6)	142(4)
C1−H1C···O2	0.900(18)	2.58(3)	3.313(6)	139(4)
C3−H3B···O1	1.08(4)	2.37(4)	3.410(7)	162(4)
C3−H3B···O2	1.08(4)	2.49(5)	3.294(7)	131(4)
3				
N1−H4A···N1	0.82(2)	2.68(3)	3.3988(6)	148(3)
N1−H4B···O2	0.82(2)	2.46(2)	3.256(3)	167(4)
N1−H4C···O1	0.82(2)	2.35(2)	3.159(3)	175(4)
N1−H4C···O2	0.82(2)	2.66(3)	3.362(3)	145(4)
C1−H1C···O2	0.960(19)	2.51(4)	3.261(3)	135(4)
C1−H1A···O1	0.959(19)	2.54(3)	3.374(3)	145(4)
C3−H3B···O1	0.89(5)	2.44(5)	3.311(4)	165(5)
C3−H3B···O2	0.89(5)	2.53(5)	3.212(4)	134(5)

CHEMISTRY
AN ASIAN JOURNAL

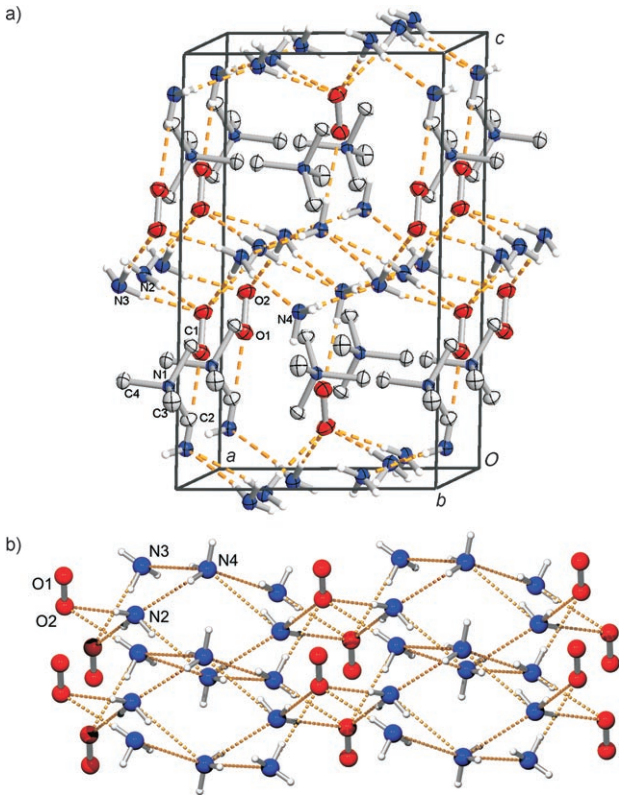

Figure 1. a) Crystal structure of **1a** viewed along [010] (thermal-displacement parameters are drawn at the 50% probability level, methyl hydrogen atoms are omitted for clarity) emphasizing the hydrogen-bonding network (dotted orange lines). The analogy to the sodium chloride packing is apparent from comparison of the relative positions of cations and anions in adjacent ion layers. b) Hydrogen-bonding layer of ribbons of ammonia molecules connected by superoxide ions in **1a**.

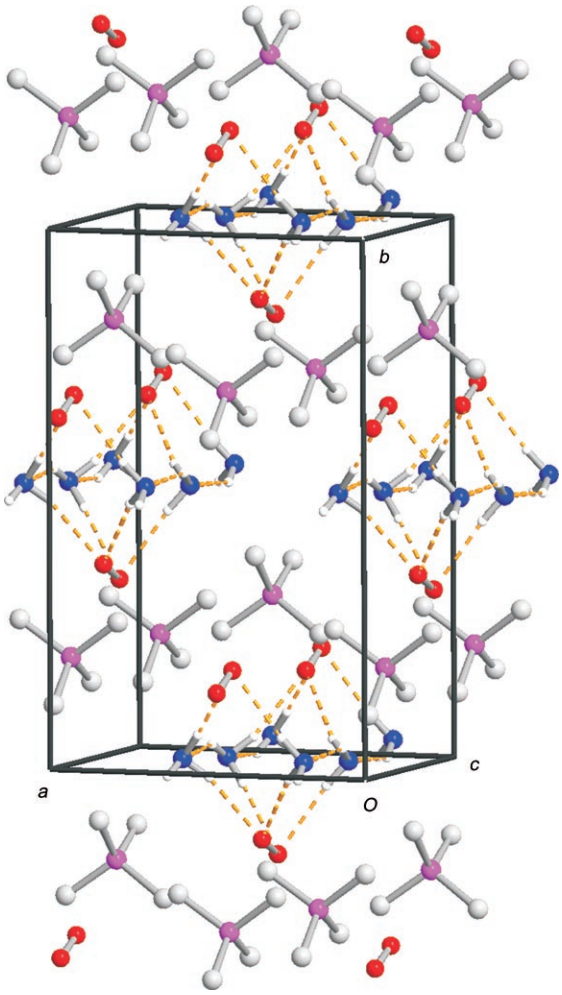

Figure 2. Crystal structure of **2** and **3** viewed along [001] illustrating the network of hydrogen bonds between the ammonia molecules and the superoxide ion along this axis (dotted orange lines; methyl hydrogen atoms are omitted for clarity).

uted to the increased size of the tetramethylphosphonium and tetramethylarsonium ions.

The O–O bond lengths in the superoxide ion in all three compounds are in the rather narrow range of 1.315(5)–1.320(3) Å. These bond lengths compare well with the values obtained for other tetraorganylammonium superoxide compounds, which range from 1.312(2) Å in tetrabutylammonium superoxide ammoniate to 1.332(2) Å in trimethylphenylammonium superoxide and 1.335(3) and 1.345(3) Å in 1,3-bis(trimethylammonium)benzene disuperoxide ammoniate.[56,57] Except for trimethylphenylammonium superoxide, all these contain ammonia molecules in their structures, which are engaged in hydrogen bonding to the superoxide ions. In these latter cases, the bond length of the superoxide ion should deviate from the "ideal" value as expected for a largely unperturbed ion because of the influence of hydrogen bonds on the electron-density distribution in the superoxide ion. We therefore consider the value found in trimethylphenylammonium superoxide to be the most-reliable reference value for a superoxide ion in the solid state that is essentially unperturbed by its environment.[57] The values for the O–O bond length in **1a**, **2**, and **3** are within 0.02 Å of this reference value. Thus, the effect of the hydrogen bonds on the superoxide bond length is apparently relatively small in these cases.

As the measurements of the physical properties of tetramethylammonium superoxide were performed on the ammonia-free substance **1b**, the residue after ammonia was removed from **1**, it would be preferable to have information about its structure as well. Because the polycrystalline nature of the samples precludes a single-crystal structure analysis, the structure was solved from X-ray powder-diffraction patterns. The X-ray powder-diffraction pattern of **1b** can be indexed by assuming a rhombohedral unit cell, indicating a structural relationship with tetramethylammonium chloride.[58,59] The paucity of reflections thwarted a structure solution and, in particular, refinements of trial structures because of the unsatisfactory data to parameter ratio.[60] However, the number of parameters can be reduced by approximating both the tetramethylammonium and superoxide ions by a rigid-body approach. With this assumption and utilizing a simulated annealing algorithm, we obtained a structural model that basically matches the powder

pattern. Subsequently, only the thermal-displacement parameters were refined, and this readily gave a rather satisfactory agreement (Table 4 and Figure 3). Although it is not possible to derive the exact geometric parameters of the molecules from a structure solution obtained in this way, it is still instructive to discuss the packing arrangement. The orientation of the superoxide ion is disordered around its center of gravity. On the basis of observations made previously on the alkali-metal superoxides,[15,20] this disorder may actually be due to a hindered rotation. Each site occupied by a superoxide ion has six tetramethylammonium ions as nearest neighbors, and vice versa. The distances of the centers of gravity of the superoxide ions to the nitrogen atoms of the ordered cation are 3.92 and 4.92 Å (3-fold each). The coordination polyhedron resembles a distorted octahedron with the superoxide ion shifted off the center. This is due to three methyl groups that point into the coordination polyhedron towards the superoxide from the opposing faces of the polyhedron. Again, the packing arrangement can be derived from the sodium chloride structure (Figure 4). The distances between the centers of gravity of the superoxide ion are 5.71 (6-fold) and 6.51 Å (6-fold).

Table 4. Crystallographic data for the Rietveld refinement of **1b**.

Formula	$C_4H_{12}NO_2$	λ [Å]	1.5406
Formula weight [g mol^{-1}]	106.1	ρ_{calcd} [g cm^{-3}]	1.1176
T [K]	292	2θ range [°]	5.010-61.97
Space group	$R\,3\,m$	R_p	0.0413
Z	3	R_{wp}	0.0533
a [Å]	6.5054(3)	R_{exp}	0.0525
b [Å]	6.5054(3)	R_{Bragg}	0.0626
c [Å]	12.9055(7)	Variables	22
V [Å^3]	472.98(4)		

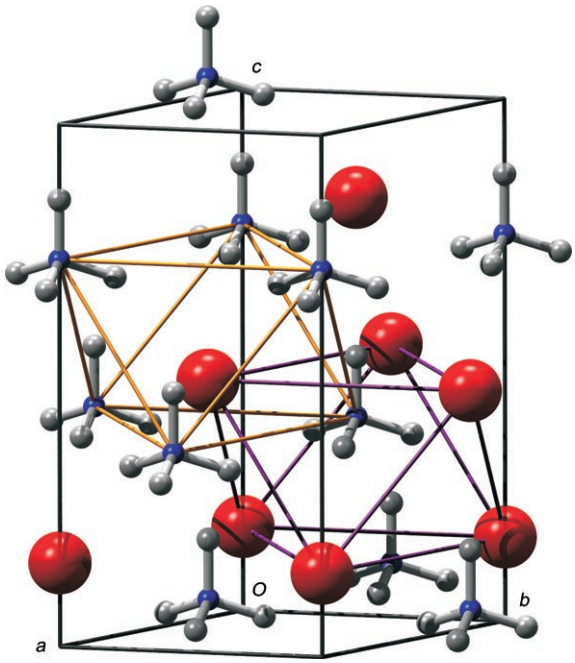

Figure 4. Cation–anion packing in **1b**. The disordered superoxide ion is symbolized by the single red sphere at the center of gravity. The six tetramethylammonium ions that surround each superoxide are connected by orange lines, and the centers of gravity of the six superoxide ions surrounding each cation by purple lines.

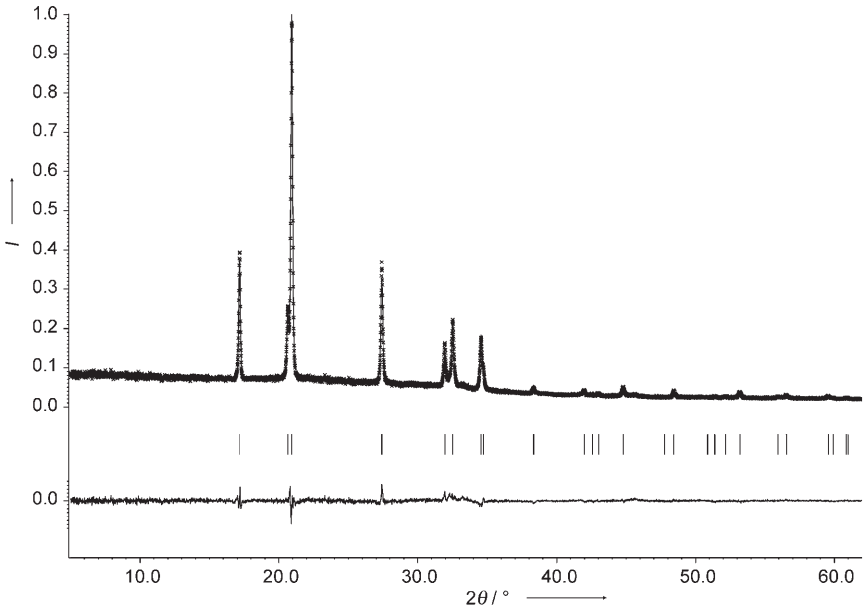

Figure 3. Rietveld refinement plot of **1b**. ×=observed pattern, ——=calculated pattern, bottom trace=difference plot, all plotted on the same scale; Bragg peaks are indicated by vertical lines.

It was reported earlier that **1b** passes through a phase transition on cooling.[60] Indeed, the powder pattern obtained at −100 °C is distinctly different from that of the high-temperature phase. Unfortunately, we were not able to index the pattern owing to significant broadening of the observed reflections.

Raman Spectroscopy

The symmetric stretching mode of the superoxide ion can be observed by Raman spectroscopy. Figure 5 shows the spectra of the desolvated samples. The presence of ammonia should show up as bands in the range 3200–3300 cm^{-1}.[64] Their absence attests that the solvent was completely removed from the samples investigated. The spectrum of **1b** displays the mode ascribed to intense vibration of the superoxide ion at 1125 cm^{-1}, a value which is in good agreement with the 1123 cm^{-1} in previous reports.[52] All the remaining vi-

CHEMISTRY
AN ASIAN JOURNAL

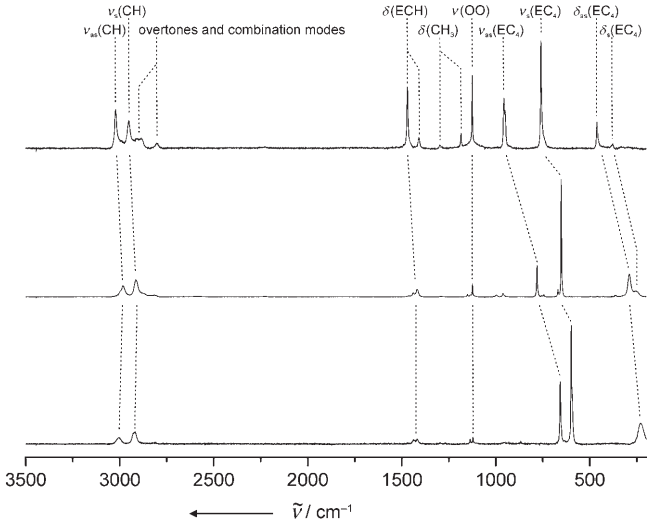

Figure 5. Raman spectra (background-corrected) of **1b** and desolvated **2** and **3** (top to bottom: E = N, P, As).

brations can be attributed to the vibrations of the tetramethylammonium ion.[65]

The spectra of tetramethylphosphonium and tetramethylarsonium superoxide are dominated by the strong bands of the symmetric and asymmetric stretch of the C_4E skeleton. Still, the superoxide vibration can be identified at 1123 and 1122 cm^{-1} for desolvated **2** and **3**, respectively. Tetramethylphosphonium superoxide contains a number of additional spurious weak vibrational bands, which do not correspond to modes of the tetramethylphosphonium cation. Some of these additional modes can be attributed to vibrations of the tetramethylammonium ion. This observation indicates that the ion exchange was possibly not complete for the sample studied. A number of small peaks could not be assigned, which may be linked with the observation of a weak evolution of gas during the synthesis that could be indicative of some decomposition.

Together with the data on the previously reported tetraorganylammonium superoxides,[52,56,57,66] there emerges a range of 1117–1131 cm^{-1} for the symmetric O–O stretching vibration of the superoxide ion, if the counterion is a large quaternary organic cation. The electrostatic interactions between cations and anions in such compounds appear to be minimized owing to the large size and correspondingly low charge density of the cation. This conclusion complies very well with the trend observed for the shift in frequency of the symmetric stretching vibration with decreasing electrostatic interaction between the superoxide ion and its environment. In the alkali-metal superoxides, this frequency decreases with increasing size of the alkali-metal cation from 1164 cm^{-1} in sodium superoxide to 1136 cm^{-1} in cesium superoxide.[21,24,30] Even lower values in the range of 1094–1114 cm^{-1} were observed for matrix-isolated alkali-metal superoxides,[67–71] and for the free superoxide ion, a value of 1090 cm^{-1} was suggested.[72]

Magnetic Susceptibility and Electron Paramagnetic Resonance of Tetramethylammonium Superoxide

The superoxide ion is a radical anion. In the gas phase, it contains three electrons in two degenerate nonbonding π_g orbitals. The magnetic moment of the superoxide ion is expected to be influenced by spin-orbit coupling due to the unequal occupation of the two degenerate orbitals.[29] The degeneracy of these orbitals is removed in the solid state, but not sufficiently to quench the orbital momentum completely. Consequently, the magnetic moments found in the alkali-metal superoxides and a number of other tetraorganyl superoxides were found to be somewhat larger than expected for a spin-only moment. Deviations from spin-only behavior and from the free-electron g factor can be studied by following the average g factor, $g_{av,}$ by powder electron paramagnetic resonance (EPR) experiments. The effective magnetic moment, μ_{eff}, is then given by Equation (1).

$$\mu_{eff} = g_{av}\sqrt{S(S+1)} \quad (1)$$

The desolvated tetramethylammonium superoxide **1b** exhibits paramagnetic behavior in the complete temperature range of 2–290 K investigated. The plot of inverse molar susceptibility versus temperature is linear over a wide temperature range and can be fitted with the Curie–Weiss law with an effective magnetic moment $\mu_{eff} = 1.66(3)\ \mu_B$ and a Weiss parameter θ of −13(2) K (Figure 6) above 75 K. Below this

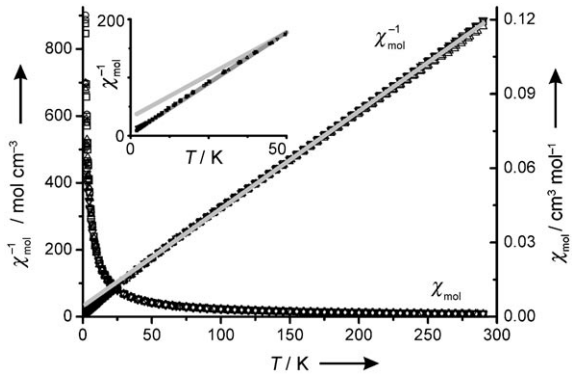

Figure 6. Temperature dependence of the magnetic susceptibility and inverse magnetic susceptibility of **1b**: representative fit of the Curie–Weiss law above 50 K (light-grey line) and below 50 K (inset, dark-grey line); ○ = 0.1 T, □ = 1 T, △ = 3 T, ▽ = 5 T.

temperature, a bend occurs in the progression of the inverse molar susceptibility with decreasing temperature. Below 50 K, the susceptibility conforms again to the Curie–Weiss law with $\mu_{eff} = 1.52(1)\ \mu_B$ and $\theta = -1(1)$ K. The high-temperature magnetic moment is close to the spin-only value and significantly lower than the previously reported single-point room-temperature value of 1.89(5) μ_B for $[N(CH_3)_4](O_2)$.[53] It also falls below the value of 1.86(2) μ_B found for trimethylphenylammonium and tetrabutylammonium superoxide.[57] The negative Weiss parameter indicates predominant

antiferromagnetic interactions between the superoxide ions, which is also different from the behavior of $[N(CH_3)_3(C_6H_5)](O_2)$ and $[N(C_4H_9)_4](O_2)$, the susceptibility of which follows the Curie law (i.e., $\theta = 0$) down to 2 K.

An analysis of the nearest-neighbor distances of the centers of gravity of the superoxide ion in trimethylphenylammonium superoxide reveals that there are four close superoxide ions at a distance of 5.54 and 6.19 Å (twofold each). The next-nearest neighbors are found at 7.05 and 7.18 Å (again twofold each), the two further superoxide units follow at 7.71 Å, and there are four more separations in the range of 8–9 Å. Intriguingly, the two closest contacts are slightly shorter than those found in **1b**. Thus, the occurrence of (albeit weak) exchange interaction effects in **1b**, and their absence in $[N(CH_3)_3(C_6H_5)](O_2)$, indicates that the consideration of the superoxide–superoxide distance alone is not sufficient to understand this finding. Different bond angles and an increased number of such short bonds in **1b** may also be of importance.

The EPR spectra of **1b** are temperature-dependent (Figure 7). At 10 K, the spectral curve contains two maxima

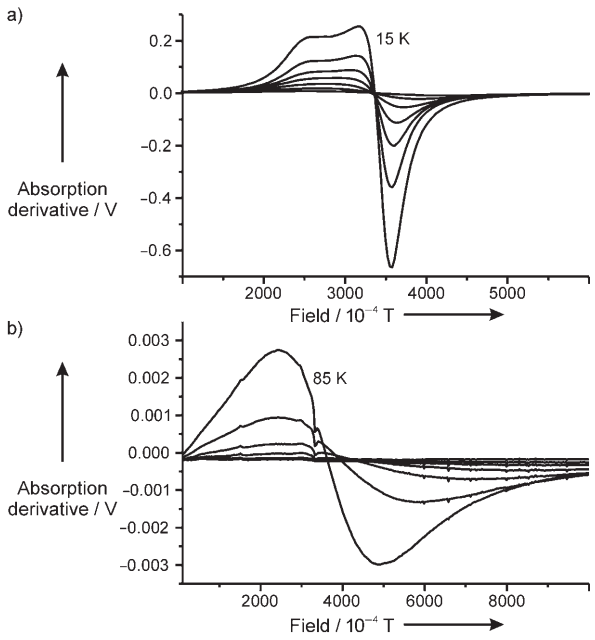

Figure 7. EPR spectra of **1b** in the temperature range a) 15–75 K and b) 85–145 K in steps of 10 K (note the different scales of the abscissa).

and one minimum as is expected for an axially symmetric g tensor. The linewidth increased markedly with increasing temperature. As a consequence, the lineshape is approximately isotropic above 60 K. At 100 K, the resonance line is even wider than the scanned field range (0–1 T). Concurrent with these changes, the maximum intensity decreased rapidly. The signal amplitude at 85 K was already two orders of magnitude smaller than at 15 K, and the weak cavity background signal was clearly visible at 95 K. The sample signal completely vanished above 140 K. These changes in signal characteristics are much more pronounced than in the related compounds, trimethylphenylammonium and tetrabutylammonium superoxide.

The spectra up to 70 K are best approximated by assuming an axially symmetric g tensor, and the average g factor was calculated from the components $g_x \approx g_y$ and g_z. At higher temperatures, the spectra were fitted to an isotropic Lorentzian function and a single g_{av} value (see Supporting Information, Figure S1). The average g factor g_{av} varied very little with the temperature in the range 10–50 K. Above 50 K it decreased markedly towards higher temperatures, from a value of 2.13 at 50 K to 1.66 at 100 K (Table 5 and Figure S2). This result is quite unexpected because, again,

Table 5. Values of the g factor obtained from fitting of the EPR spectra of **1b**.

T	Anisotropic fit				Isotropic fit
[K]	g_x	g_y	g_z	g_{av}	g_{av}
10	1.903	1.902	2.655	2.155	
15	1.903	1.920	2.636	2.153	
20	1.897	1.909	2.647	2.151	
25	1.898	1.924	2.623	2.148	
35	1.884	1.928	2.623	2.145	
40	1.884	1.917	2.604	2.135	
45	1.892	1.901	2.614	2.136	
50	1.877	1.905	2.614	2.132	
55	1.880	1.881	2.580	2.114	
60	1.890	1.890	2.619	2.133	
65	1.857	1.867	2.442	2.055	1.995
70	1.826	1.838	2.407	2.024	1.977
75	1.800	1.806	2.231	1.946	1.944
80	1.727	1.760	2.186	1.891	1.903
85	1.657	1.657	2.030	1.781	1.825
90					1.783
95					1.688
100					1.663

tetramethylammonium superoxide behaves differently to its relatives trimethylphenylammonium and tetrabutylammonium superoxide, for which the g factor was approximately constant in the range 10–110 K and of similar magnitude as the g_{av} value of **1b** below 60 K.[57] On the other hand, such a small g value in the temperature range around and above 100 K is in accord with the surprisingly low effective magnetic moment of **1b** even if the orbital momentum is not quenched, as indicated by calculating the splitting of the energy levels from the EPR data (see Supporting information).

The most-significant structural difference between tetramethylammonium and trimethylphenylammonium superoxide is the rotational reorientation of the superoxide ion in **1b**. As the rotation of an ion is a cyclic motion, it gives rise to an orbital momentum,[73–75] which by coupling with the intrinsic electronic properties of the superoxide ion may result in the observed and significantly lower-than-expected g factor. This interpretation that the smaller g factor is caused by the molecular motion of the superoxide ion is supported by the observation that the g factor changes only very little

CHEMISTRY
AN ASIAN JOURNAL

with temperature below 60 K, at which the rotational motion is essentially frozen.

Conclusions

We have shown that the ion-exchange reaction not only applies to the synthesis of tetraorganylammonium superoxides, it also enables the synthesis of tetramethylphosphonium and tetramethylarsonium superoxide. Even though the tetramethylonium ions $[E(CH_3)_4]^+$ (E = N, P, As) deviate from the perfectly spherical shape of the alkali-metal ions, they are not sufficiently aspherical to pack tightly enough with the dumbbell-shaped superoxide ion to preclude incorporation of additional solvent ammonia molecules into the crystal structure. Upon removal of the ammonia in the crystal, polycrystalline samples were obtained. In the resulting crystal structure of solvent-free tetramethylammonium superoxide, the superoxide ion is rotationally disordered. The effective magnetic moment of tetramethylammonium superoxide is substantially smaller than those observed in tetraorganylammonium superoxides containing larger substituent groups at the nitrogen atom of the cation. Concurrently, the *g* factor has a temperature dependence that results in a smaller value above 60 K. We ascribe this finding to molecular rotation of the superoxide ion around its center of gravity.

Experimental Section

General

Caution! Superoxide salts with organic cations are potentially explosive, and organic compounds of arsenic are classified as human carcinogens. They should be handled with appropriate care and in small amounts only. All operations were carried out under either vacuum or a dry argon atmosphere using standard Schlenk techniques. Ammonia (grade 3.8, Messer–Griesheim) was liquefied and stored over potassium metal at −78 °C.

Syntheses

Potassium superoxide was prepared by oxidation of potassium metal with oxygen.[76] To prepare the ion-exchange resin for the synthesis of tetramethylphosphonium and tetramethylarsonium superoxide, tetramethylphosphonium bromide (98 %+, Chempur) and tetramethylarsonium iodide, which was prepared according to procedures described in the literature,[77] were each dissolved in methanol (HPLC grade, Riedel-deHaën) and converted into the corresponding hydroxide by vigorous stirring with freshly precipitated silver oxide for 2 h. After filtration, 0.9 mol (active sites) of the acidic form of the ion-exchange resin (Amberlyst 15, Merck) was added to these solutions. The ion-exchange resin was separated from the solution by filtration after a typical period of five days. It was washed several times with methanol and thoroughly dried at 105 °C in a dynamic vacuum.

1b: Tetramethylammonium hydroxide pentahydrate (99 %, Acros) was dried to the monohydrate and converted into tetramethylammonium superoxide by metathesis reaction with potassium superoxide.[53,78] Tetramethylammonium hydroxide monohydrate (0.3–0.5 g, 2.7–4.5 mmol) and an excess of potassium superoxide of at least 3.5-fold (0.672–1.2 g) were ground, and mixed for reaction in an evacuated H-shaped Schlenk vessel, whose two sides were connected by glass filter sieves of porosity 3, for three days. The oxygen released in the reaction $[N(CH_3)_4]OH{\cdot}H_2O + 3KO_2 \rightarrow [N(CH_3)_4](O_2) + 3KOH + {}^3/_2O_2$ was removed once a day by evacuation. In the final step of the synthesis, tetramethylammonium superoxide was separated from potassium hydroxide and superfluous potassium superoxide by repeated extraction (three times) with liquid ammonia (≈20 mL). To improve the purity of the product, it was recrystallized from ammonia. On evaporation of the solvent from highly concentrated solutions, **1a** first crystallized in the form of long colorless needles. These become opaque after total removal of the solvent at −33 °C. Application of a dynamic vacuum yielded the ammonia-free **1b**.

2: The ion-exchange resin (1.0 g, 4.6 mmol equiv) was placed in one leg of an H-shaped glass apparatus whose two sides were connected by a glass filter sieve of porosity 3. At −78 °C, tetramethylammonium superoxide (0.0791 g, 0.74 mmol) was added to the ion-exchange resin. Some evolution of gas was observed during the condensation of ammonia (≈25 mL) into the reaction vessel. This mixture was allowed to react for 24 h at −50 °C, after which it was separated from the ion-exchange resin by filtration into the other leg of the apparatus. Slow concentration of the solution yielded long colorless needles of **2**.

3: The ion-exchange resin (1.5 g, 6.9 mmol equiv) was placed in one leg of an H-shaped glass apparatus. At −78 °C, tetramethylammonium superoxide (0.1121 g, 1.05 mmol) was added to the ion-exchange resin. Then, ammonia (≈25 mL) was condensed into the reaction vessel. The solution was warmed once to −35 °C to dissolve the tetramethylammonium superoxide and allowed to react for 24 h at −50 °C. Subsequently, it was separated from the ion-exchange resin by filtration into the other leg of the apparatus. Slow evaporation of the ammonia yielded long colorless needle-shaped crystals of **3** when the concentrated solution was cooled to −78 °C.

X-ray Crystallography

Crystals of **1a**, **2**, and **3** were selected under a microscope from an inert oil (perfluorinated polyether Galden, Ausimont) cooled in a stream of nitrogen gas to −50 °C.[79] They were transferred to the inert oil in their mother liquor and picked up with a nylon loop attached to the goniometer head (Hampton Research), transferred into liquid nitrogen, and mounted onto the diffractometer in a cooling N_2 stream. The intensities of the Bragg reflections were measured at −173 °C with a Bruker AXS Smart Apex diffractometer using $Mo_{K\alpha}$ radiation.

The structure solution and parameter refinement was performed with the SHELX97 software suite.[80] The parameters were refined by using full-matrix least squares against $|F|^2$. All non-hydrogen atomic parameters were refined allowing for anisotropic displacement. Hydrogen atoms were located by inspection of difference electron-density maps. Positional parameters of the hydrogen atoms were refined freely for **1a**. For **2** and **3**, they were restrained to equal distances of the atoms from the non-hydrogen atom they are bonded to and from each other. Isotropic thermal-displacement parameters were refined freely for the hydrogen atoms in **1a** and for the ammonia hydrogen atoms in **2** and **3**. The thermal-displacement parameters of the methyl hydrogen atoms in **2** were confined to a value proportional to the isotropic thermal displacement of the carbon atom they are attached to. In **3**, the parameters were restrained to a common value for all methyl hydrogen atoms.

Powder X-ray data of **1b** were collected on a Stoe StadiP diffractometer with monochromatic $Cu_{K\alpha}$ radiation and a linear position-sensitive detector and a step width of 0.01°. Variable count rates were employed to obtain good statistics for the weak reflections in the high-angle range. The structure of **1b** was solved by global optimization in direct space with the DASH structure-solution package.[81] The measured powder pattern was subjected to Pawley refinement in the space group *R*3*m* to extract correlated integrated intensities. The tetramethylammonium and superoxide moieties were described as rigid bodies with internal coordinates constructed by using bond lengths and angles from the structure refinement of **1a**. The optimized structure was validated by Rietveld refinement with the JANA2000 program,[82] with the fractional coordinates obtained at the end of the simulated annealing run kept fixed and the isotropic thermal-displacement parameters allowed to refine.

CCDC-604494–604497 (**1a**, **1b**, **2**, and **3**, respectively) contain the supplementary crystallographic data for this paper. These data can be obtained free of charge from the Cambridge Crystallographic Data Centre, 12

Union Road, Cambridge CB2 1EZ, UK (fax: (+44) 1223-336-033; e-mail: deposit@ccdc.cam.ac.uk) or at www.ccdc.cam.ac.uk/conts/retrieving.html.

Raman Spectroscopy

Raman spectra in the range 200–3500 cm^{-1} were recorded at room temperature with a Jobin Yvon Horiba laser Raman microscope spectrometer-type Labram that employed a He/Ne laser ($\lambda = 632.8$ nm). The samples were sealed in capillaries with a diameter of 1 mm under dry argon and kept at −78 °C until the time of measurement.

Magnetic Susceptibility

Data for **1b** was recorded with a MPMS7 Quantum Design SQUID magnetometer at magnetic fields of 0.1, 1, 3, and 5 T in the temperature range 2–290 K. Powder samples were sealed in Suprasil quartz glass tubes filled with helium gas to enable rapid thermal equilibration. The data were corrected for the magnetization of the empty sample holders and for the diamagnetic contributions of the constituent ions by using Pascal increments, which summed up to $-71\times10^{-6}\,cm^3\,mol^{-1}$. The corrected magnetic susceptibilities were then analyzed by fitting to the Curie–Weiss law $\chi_{exp} = C/(T-\Theta)$, with $C = \mu_0 N_A \mu^2/3k$, above 100 K and below 50 K, respectively. The values of the effective magnetic moments and Weiss parameters for all fields were then averaged. The weighing error was taken into account in calculating the standard deviations of the effective magnetic moment. We repeated the measurement on five samples from different batches of substance. All in all, the effective magnetic moments agree within $\pm 0.08\ \mu_B$ of the value reported herein.

EPR Spectroscopy

EPR spectra were recorded on a Bruker ER040XK microwave X-band spectrometer and a Bruker BE25 magnet equipped with a BH15 field controller calibrated against diphenylpicrylhydrazyl (DPPH). Spectra for **1b** were recorded in the temperature range 10–150 K in steps of 5 K. Samples were sealed in Suprasil quartz glass ampoules and cooled in an Oxford Instruments ESR 910 continuous-flow He cryostat. The spectra were fitted with the Powfit program in the NIEHS public EPR software package by refining the diagonal g tensor components g_x, g_y, and g_z and parallel and perpendicular linewidths in the temperature range 10–85 K.[83] The lineshape was found to be approximately symmetric above 60 K. The spectra were fitted to a single Lorentzian line according to Equation (2):

$$I = -2I_0\left(\frac{\Delta H^2(H-H_0)}{\left(\Delta H^2+(H-H_0)^2\right)^2}+\frac{\Delta H^2(H+H_0)}{\left(\Delta H^2+(H+H_0)^2\right)^2}\right)+B_0+B_1H+B_2H^2 \quad (2)$$

up to a temperature of 100 K, above which the fit results became unreliable due to low intensity and large signal width. The refined parameters I_0, ΔH, and H_0 describe the signal, and the background is modeled by the parameters B_0, B_1, and B_2. The background contribution has a significant effect on the value of H_0 only for spectra in the range 90–100 K. The value of g_{av} was obtained from the resonance condition $h\nu = g_{av}\mu_B H_0$ with the microwave frequency $\nu = 9.2847\times10^9$ Hz.

Acknowledgements

We thank Sanela Kevrić for assistance with the preparative work, Eva Brücher for the magnetic-susceptibility measurements, and Dr. Hans Vogt for recording the Raman spectra.

[1] L. Vaska, *Acc. Chem. Res.* **1976**, *9*, 175–183.
[2] M. H. Gubelmann, A. F. Williams, *Struct. Bonding (Berlin)* **1983**, *55*, 2–65.
[3] *Oxygen Complexes and Oxygen Activation by Transition Metal Complexes*, (Eds.: A. E. Martell, D. T. Sawyer), Plenum Press, New York, **1988**.
[4] I. M. Klotz, D. M. Kurtz, *Chem. Rev.* **1994**, *94*, 567–568.
[5] C. J. Cramer, W. B. Tolman, K. H. Theopold, A. L. Rheingold, *Proc. Natl. Acad. Sci. USA* **2003**, *100*, 3635–3640.
[6] I. I. Vol'nov, Peroxides, *Superoxides, and Ozonides of Alkali and Alkaline Earth Metals*, Plenum Press, New York, **1966**.
[7] W. Hesse, M. Jansen, W. Schnick, *Prog. Solid State Chem.* **1989**, *19*, 47–110.
[8] N. Korber, W. Assenmacher, M. Jansen, *Prax. Naturwiss. Chem* **1991**, *40*, 18–24.
[9] W. Kassatochkin, W. Kotow, *J. Chem. Phys.* **1936**, *4*, 458.
[10] S. E. Stephanou, W. H. Schechter, W. J. Argersinger, Jr., J. Kleinberg, *J. Am. Chem. Soc.* **1949**, *71*, 1819–1821.
[11] W. H. Schechter, J. K. Thompson, J. Kleinberg, J. *J. Am. Chem. Soc.* **1949**, *71*, 1816–1818.
[12] D. H. Templeton, C. H. Dauben, *J. Am. Chem. Soc.* **1950**, *72*, 2251–2254.
[13] E. Seyb, J. Kleinberg, *J. Am. Chem. Soc.* **1951**, *73*, 2308–2309.
[14] G. S. Zhdanov, Z. V. Zvonkova, *Dokl. Akad. Nauk SSSR* **1952**, *82*, 743–746.
[15] G. F. Carter, D. H. Templeton, *J. Am. Chem. Soc.* **1953**, *75*, 5247–5249.
[16] S. C. Abrahams, J. Kalnajs, *Acta Crystallogr.* **1955**, *8*, 503–506.
[17] J. E. Bennett, D. J. E. Ingram, M. C. R. Symons, P. George, J. S. Griffith, *Philos. Mag.* **1955**, *46*, 443–444.
[18] E. G. Brame, S. Cohen, J. L. Margrave, V. W. Meloche, *J. Inorg. Nucl. Chem.* **1957**, *4*, 90–92.
[19] A. D. McLachlan, M. C. R. Symons, M. G. Townsend, *J. Chem. Soc.* **1959**, 952–957.
[20] F. Halverson, *Phys. Chem. Solids* **1962**, *23*, 207–214.
[21] J. A. Creighton, E. R. Lippincott, *J. Chem. Phys.* **1964**, *40*, 1779–1780.
[22] J. T. Sparks, T. Komoto, *J. Appl. Phys.* **1966**, *37*, 1040–1041.
[23] H. G. Smith, R. M. Nicklow, L. J. Raubenheimer, M. K. Wilkinson, *J. Appl. Phys.* **1966**, *37*, 1047–1049.
[24] F. J. Blunt, P. J. Hendra, J. R. Mackenzie, *J. Chem. Soc. D Chem. Commun.* **1969**, 278–279.
[25] J. B. Bates, M. H. Brooker, G. E. Boyd, *Chem. Phys. Lett.* **1972**, *16*, 391–395.
[26] M. Bösch, W. Känzig, *Helv. Phys. Acta* **1973**, *46*, 17.
[27] M. Bösch, W. Känzig, *Phys. Kondens. Mater.* **1973**, *16*, 107–112.
[28] V. Y. Dudarev, A. B. Tsentsiper, M. S. Dobrolyubova, *Sov. Phys. Crystallogr.* **1974**, *18*, 477–479.
[29] A. Zumsteg, M. Ziegler, W. Känzig, M. Bösch, *Phys. Condens. Matter* **1974**, *17*, 267–291.
[30] M. Bösch, W. Känzig, *Helv. Phys. Acta* **1975**, *48*, 743–785.
[31] A. U. Khan, S. D. Mahanti, *J. Chem. Phys.* **1975**, *63*, 2271–2278.
[32] M. Ziegler, H. R. Meister, W. Känzig, *Helv. Phys. Acta* **1975**, *48*, 599–607.
[33] S. D. Mahanti, A. U. Khan, *Solid State Commun.* **1976**, *18*, 159–162.
[34] M. Ziegler, M. Rosenfeld, W. Känzig, P. Fischer, *Helv. Phys. Acta* **1976**, *49*, 57–90.
[35] M. Rosenfeld, M. Ziegler, W. Känzig, *Helv. Phys. Acta* **1978**, *51*, 298–320.
[36] M. Labhart, D. Raoux, W. Känzig, *Helv. Phys. Acta* **1977**, *50*, 602–603.
[37] M. Labhart, D. Raoux, W. Känzig, M. A. Bösch, *Phys. Rev. B* **1979**, *20*, 53–70.
[38] G. Kemeny, S. D. Mahanti, *Phys. Rev. B* **1979**, *20*, 2961–2963.
[39] S. D. Mahanti, G. Kemeny, *Phys. Rev. B* **1979**, *20*, 2105–2117.
[40] M. A. Bösch, M. E. Lines, M. Labhart, *Phys. Rev. Lett.* **1980**, *45*, 140–143.
[41] G. Kemeny, T. A. Kaplan, S. D. Mahanti, D. Sahu, *Phys. Rev. B* **1981**, *24*, 5222–5228.
[42] M. E. Lines, M. A. Bösch, *Phys. Rev. B* **1981**, *23*, 263–270.
[43] M. E. Lines, *Phys. Rev. B* **1981**, *24*, 5248–5259.
[44] S. Biljana, *Thermochim. Acta* **1985**, *92*, 231–234.

[45] E. Bertel, F. P. Netzer, G. Rosina, H. Saalfeld, *Phys. Rev. B* **1989**, *39*, 6082–6086.
[46] M. Pedio, M. Benfatto, S. Aminpirooz, J. Haase, *Europhys. Lett.* **1993**, *21*, 239–244.
[47] R. M. Kadam, M. D. Sastry, *Phase Transitions* **1997**, *60*, 79–87.
[48] T. R. Krawietz, D. K. Murray, J. F. Haw, *J. Phys. Chem. A* **1998**, *102*, 8779–8785.
[49] H. D. B. Jenkins, H. K. Roobottom, J. Passmore, L. Glasser, *Inorg. Chem.* **1999**, *38*, 3609–3620.
[50] A. D. McElroy, J. S. Hashman, *Inorg. Chem.* **1964**, *3*, 1798–1799.
[51] E. I. Latysheva, É. N. Cherkasov, S. A. Tokareva, N. G. Velikova, I. I. Vol'nov, *Bull. Acad. Sci. USSR Div. Chem. Sci. (Engl. Transl.)* **1974**, *23*, 1610–1612.
[52] D. T. Sawyer, T. S. Calderwood, K. Yamaguchi, C. T. Angelis, *Inorg. Chem.* **1983**, *22*, 2577–2583.
[53] K. Yamaguchi, T. S. Calderwood, D. T. Sawyer, *Inorg. Chem.* **1986**, *25*, 1289–1290.
[54] W. Hesse, M. Jansen, *Angew. Chem.* **1988**, *100*, 1388–1389; *Angew. Chem. Int. Ed. Engl.* **1988**, *27*, 1341–1342.
[55] W. Hesse, M. Jansen, *Inorg. Chem.* **1991**, *30*, 4380–4385.
[56] H. Seyeda, M. Jansen, *J. Chem. Soc. Dalton Trans.* **1998**, 875–876.
[57] P. D. C. Dietzel, R. K. Kremer, M. Jansen, *J. Am. Chem. Soc.* **2004**, *126*, 4689–4696.
[58] M. Stammler, *J. Inorg. Nucl. Chem.* **1967**, *29*, 2203–2221.
[59] C. W. F. T. Pistorius, A. A. V. Gibson, *J. Solid State Chem.* **1973**, *8*, 126–131.
[60] W. Hesse, *PhD thesis*, Universität Bonn (Germany), **1990**.
[61] J. Jander, *Anorganische und allgemeine Chemie in flüssigem Ammoniak*, Vieweg, Braunschweig, **1966**.
[62] D. Nichols, *Inorganic Chemistry in Liquid Ammonia*, Elsevier, Amsterdam, **1979**.
[63] R. Boese, N. Niederprüm, D. Bläser, A. Maulitz, M. Y. Antipin, P. R. Mallinson, *J. Phys. Chem. B* **1997**, *101*, 5794–5799.
[64] K. R. Plowman, J. J. Lagowski, *J. Phys. Chem.* **1974**, *78*, 143–148.
[65] Z. Deng, D. E. Irish, *J. Phys. Chem.* **1994**, *98*, 11169–11177.
[66] H. Seyeda, *PhD thesis*, Universität Bonn (Germany), **1998**.
[67] R. R. Smardzewski, L. Andrews, *J. Chem. Phys.* **1972**, *57*, 1327–1333.
[68] L. Andrews, R. R. Smardzewski, *J. Chem. Phys.* **1973**, *58*, 2258–2261.
[69] L. Andrews, J.-T. Hwang, C. Trindle, *J. Phys. Chem.* **1973**, *77*, 1065–1073.
[70] R. R. Smardzewski, L. Andrews, *J. Phys. Chem.* **1973**, *77*, 801–804.
[71] H. M. Himmel, A. J. Downs, T. M. Greene, *Chem. Rev.* **2002**, *102*, 4191–4241.
[72] W. Holzer, W. F. Murphy, H. J. Bernstein, J. Rolfe, *J. Mol. Spectrosc.* **1968**, *26*, 543–545.
[73] W. H. Flygare, *Chem. Rev.* **1974**, *74*, 653–687.
[74] J. F. Ogilvie, J. Oddershede, S. P. A. Sauer, *Adv. Chem. Phys.* **2000**, *111*, 475–536.
[75] D. Ceresoli, E. Tosatti, *Phys. Rev. Lett.* **2002**, *89*, 116402/1–116402/4.
[76] G. Brauer, *Handbuch der präparativen anorganischen Chemie*, Ferdinand-Enke Verlag, Stuttgart, **1978**.
[77] W. Assenmacher, M. Jansen, *Z. Anorg. Allg. Chem.* **1995**, *621*, 143–148.
[78] D. S. Bohle, E. S. Sagan, W. H. Koppenol, R. Kissner, *Inorg. Synth. Inorg. Syn.* **2004**, *34*, 36–42.
[79] D. Stalke, *Chem. Soc. Rev.* **1998**, *27*, 171–178.
[80] G. Sheldrick, SHELXS97 and SHELXL97: Program Suite for the Solution and Refinement of Crystal Structures, University of Göttingen (Germany), **1997**.
[81] W. I. F. David, K. Shankland, N. Shankland, *Chem. Commun.* **1998**, 931–932.
[82] V. Petricek, M. Dusek, Jana2000: Structure-Determination Software Programs, Institute of Physics, Praha (Czech Republic), **2000**.
[83] G. P. Lazos, B. M. Hoffmann, C. G. Franz, POWFIT: Program for Fitting and Simulating Anisotropic ESR Spectra, QCPE program number 265, Quantum Chemistry Program Exchange, Indiana University, Bloomington, IN.

Received: September 6, 2006
Published online: December 12, 2006

